Search for superheavy elements with $292 \leqslant A \leqslant 310$ in nature with accelerator mass spectrometry

P. Ludwig,[1,*] T. Faestermann,[1] G. Korschinek,[1] G. Rugel,[1,†] I. Dillmann,[1,‡] L. Fimiani,[1] S. Bishop,[1] and P. Kumar[1,2]

[1]*Physik Department, Technische Universität München, D-85748 Garching, Germany*

[2]*AMS Group, Inter-University Accelerator Centre (IUAC), New Delhi 110067, India*

There is a possibility that small traces of long-lived superheavy elements ($Z \geqslant 104$) still exist in nature. An ultrasensitive search for such superheavy elements has been conducted at the Maier-Leibnitz Laboratory in Garching (Germany) by means of accelerator mass spectrometry. A sample of raw platinum has been scanned for 13 different masses in the range $292 \leqslant A \leqslant 310$. The masses $A = 292$ and 298 were scanned in pure osmium and pure lead fluoride, respectively. For each mass, several hours of background-free data were recorded. Since no events could be attributed to superheavy elements, upper limits on their abundances in the sample materials on the order of 10^{-14}–10^{-16} were established.

I. INTRODUCTION

For several decades, it has been speculated that there exists a region in the chart of nuclides beyond the valley of stability containing long-lived or even stable, very neutron-rich isotopes of superheavy elements (SHEs). This region is referred to as the island of stability. The artificial creation of these extremely neutron-rich nuclei in laboratory fusion-evaporation reactions is hindered by the extremely small cross sections and also by the lack of stable target-projectile combinations neutron-rich enough to reach the theoretical island of stability. The heaviest synthetically produced isotope so far, ^{294}118 with $N = 176$, was produced with the three-neutron evaporation channel of the reaction ^{249}Cf + ^{48}Ca, [1] which is still some distance from the well-established spherical shell closure at $N = 184$ [2,3]. Heavier neutron-rich target-beam combinations were up to now unsuccessful. The gap to $N = 184$ becomes bigger for SHEs with lower Z, e.g., the heaviest synthetically produced isotope of hassium ($Z = 108$), ^{277}Hs [4], has only 169 neutrons. This means that the nuclear properties of nuclei situated close to or on the island of stability have to be estimated by theory, while the elemental properties can be obtained using a combination of theoretical predictions and, if available, experimental data on their less neutron-rich isotopes. For a more detailed review on this topic, the reader is referred to the work of Oganessian [5].

A completely different approach to SHEs is the search for them in nature. It is possible that small amounts of SHEs are still present in nature if they were synthesized in sufficient amounts in the rapid neutron capture process (r process; see e.g. Ref. [6]) and if their half-lives are sufficiently long (in excess of 10^8 years). The most promising candidates are doubly magic nuclei, due to the increased stability provided by shell effects. While the spherical neutron shell closure $N = 184$ is well established, the next spherical proton shell closure beyond $Z = 82$ (lead), assumed to lie in the range of $108 \leqslant Z \leqslant 126$, and the exact N and Z of the most stable nucleus beyond the valley of stability, are still being disputed [7,8]. If indeed SHEs have survived until today, they will undoubtedly exist only in very small traces. For several decades there have been searches for SHEs in nature using various experimental techniques, without confirmed success. The reported discovery of a SHE with $Z = 122$ and $A = 292$ in a sample of natural thorium by Marinov *et al.* [9] using inductively coupled plasma mass spectrometry (ICPMS) could not be confirmed by Dellinger *et al.* using accelerator mass spectrometry (AMS) [10] and is thus doubtful. As an ultrasensitive technique for rare isotope identification, AMS serves as a unique tool for the search for SHEs in nature, because it can reach down to isotopic ratios of 10^{-16} and even lower, as it benefits from a complete suppression of molecular background.

In this paper, we first present our approach in choosing sample materials and superheavy candidates to search for with AMS (Sec. II), followed by a description of our setup (Sec. III) and measuring technique (Sec. IV). After some considerations about uncertainties in this type of experiment (Sec. V), we present our results (Sec. VI) and conclude with an outlook (Sec. VII).

II. SHE CANDIDATES FOR AMS

Under the assumption that the SHEs created in the r process behave like their chemically lighter homologue group members during geochemical evolution, it is reasonable to search for SHEs in the respective natural samples of those homologue elements. Although there has been much progress in the determination of the chemical properties of SHEs over the last decades, uncertainties still remain. This implies that it is favorable to use a sample material consisting of several possibly chemically homologous elements for a

———————
*peter.ludwig@ph.tum.de

†Current affiliation: Helmholtz-Zentrum Dresden-Rossendorf, Postfach 510119, 01314 Dresden, Germany.

‡Current affiliation: II. Physikalisches Institut, Justus-Liebig-Universität Giessen, D-35392 Giessen, Germany and GSI Helmholtzzentrum für Schwerionenforschung GmbH, Planckstrasse 1, D-64291 Darmstadt, Germany.

FIG. 1. Shown here is an excerpt of the periodic table of elements including well known electron affinities of the elements taken from Middleton [15], and the mass fraction of the elements in the raw platinum sample obtained from Impala Platinum.

wide-spread search for SHEs in nature. To avoid losses, sample materials should have undergone no or only minor chemical processing.

The primary sample material chosen for this search was raw platinum obtained from the Impala platinum mines in South Africa [11]. This material corresponds to raw platinum before further processing in the platinum metals refinery. An excerpt of the chemical composition can be seen in Fig. 1. The chemical analysis for most elements in the material was performed by Impala (accounting for roughly 80% of the mass). This was confirmed and supplemented using electron microscopy. The observed characteristic x-ray intensities were used to calculate the remaining abundances, neglecting hydrogen. The use of raw platinum allowed us to scan for several SHEs in one sample material, because it contains different possible chemical homologues to SHEs, most importantly platinum group elements (Ru, Rh, Pd, Os, Ir, and Pt). The material, in the form of a dry powder, required no further chemical treatment for use in our ion source. In addition to scanning raw platinum for SHEs with $A = 292$, 293, 294, 295, 297, 299, 300, 301, 302, 304, 306, 308, and 310, the mass $A = 292$ was also scanned in a high purity osmium sample obtained from Alfa Aesar Europe [12] (Lot No. C21T042), because osmium has been shown to have chemical behavior similar to hassium [13,14] (element 108), with the possibly doubly magic isotope ^{292}Hs ($N = 184$). Also, a search for element 114 has been conducted in its possible chemical homologue lead in the form of lead fluoride, also obtained from Alfa Aesar (Lot No. 21397), by scanning for the isotope ^{298}114. The choice of the masses for which to scan was influenced by several factors. First, masses of the most likely chemical homologues with $N = 184$, such as ^{295}Rg because of the presence of gold in the raw platinum sample, were preferred. Second, mass settings (with corresponding choice of charge states) that provided a low but stable count

rate of low-energy ions were favored. In addition, the limited amount of beam time restricted the measurement to 14 different masses.

Considering their nucleosynthesis in the r process, which depends strongly on fission barriers and neutron separation energies, assuming equal stability, the lighter SHEs ($108 \leqslant Z \leqslant 111$ and $292 \leqslant A \leqslant 295$) are more likely to be found in nature, because their production should be favored in the r process, as suggested in calculations (see, e.g., Ref. [6]).

III. EXPERIMENTAL TECHNIQUE

For these measurements, the AMS setup at the Maier-Leibnitz Laboratory in Garching was used. A sketch of this setup can be seen in Fig. 2. Our sample materials (all powders) were hammered into copper sample holders and inserted into the ion source. The lead fluoride was mixed 1:1 (by volume) with silver powder to improve stability of the
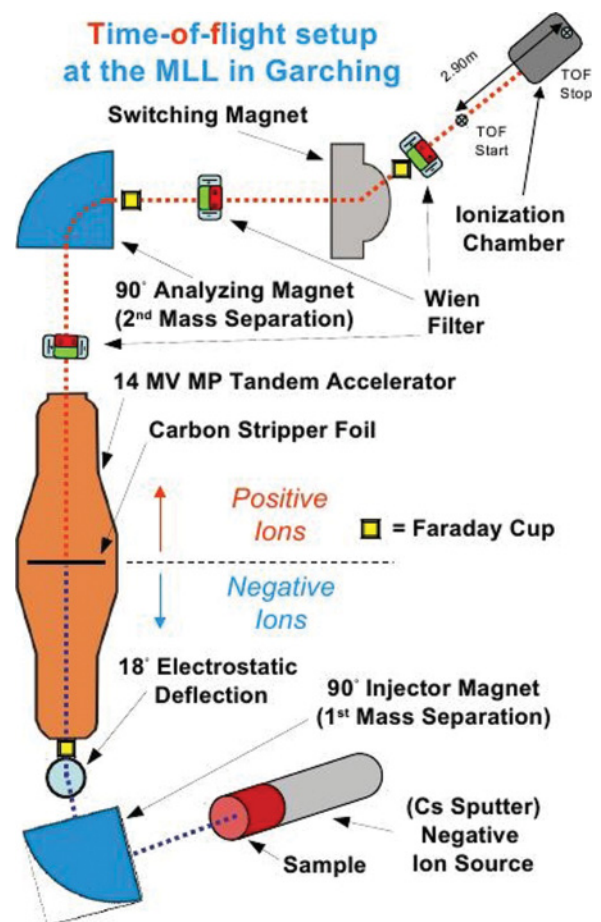

FIG. 2. (Color online) The figure shows a sketch of the main components of the time-of-flight (TOF) setup at the Maier-Leibnitz Laboratory (MLL) in Garching, featuring a Middleton-type Cs-sputter ion source, a 14-MV Tandem accelerator, three Wien filters, and an E–multi-ΔE TOF particle identification system. (Not to scale.)

ion current. The ion beam is produced by a Middleton-type cesium sputter ion source with a spherical ionizer [16]. After extraction, the negatively charged ions undergo a mass separation in a 1.2-T dipole magnet (resolution during the experiment $m/\Delta m \approx 300$) on the low-energy side of the accelerator. After passing a 150 kV preacceleration potential, the beam is injected into a 14 MV tandem accelerator. Using a single carbon stripper foil at the high voltage terminal, a distribution of positive charge states is produced. At this point all molecules are destroyed by Coulomb explosions, which eliminates any molecular background and thus allows for very clean measurements. The terminal voltage for this experiment was in the range of 8–11 MV. After further acceleration to ground potential at the high-energy side of the accelerator, the ions pass a Wien filter ($m/\Delta m \approx 80$) and another 90° analyzing magnet (1.6 T), which selects a desired value of p/q (momentum to charge ratio). After passing a second Wien filter ($m/\Delta m \approx 40$) and a switching magnet, the ions enter a dedicated AMS beamline especially designed for the detection of heavy nuclei (e.g., actinides). It features a third Wien filter ($m/\Delta m \approx 120$), a time-of-flight (TOF) detection system with a 2.9-m flight path ($m/\Delta m \approx 600$), and an ionization chamber. The start signal for the TOF measurement is generated in a microchannel plate detector (smooth carbon foil, 7.1 μg/cm^2) [17]. Through a thin mylar foil (0.9 μm), the beam then enters the ionization chamber (3–5 mbar isobutane) equipped with a split anode (two ΔE signals) and a Frisch grid, where the energy loss in the gas can be measured. The remaining energy of the ions is then measured in a surface barrier silicon detector which is mounted inside the ionization chamber and provides the stop signal for the TOF measurement [18], as well as the trigger for the data aquisition. Ions can thus be individually counted and identified by E, ΔE, and TOF. In addition, the data acquisition features a pile-up rejection system.

IV. MEASUREMENT PRINCIPLE

To perform the measurements, the optical elements on both the low- and high-energy sides of the accelerator are tuned with beams of known isotopes. To calibrate the detection system, several beams of well defined energy were used, for example ^{232}Th, ^{238}U, and ^{209}Bi. These beams were traced along the beam line using several Faraday cups and focused toward the detection system. During and after this calibration, the magnetic components on the high-energy side of the accelerator remain unchanged, only allowing ions of well known magnetic rigidity to arrive at the detection system. The injector magnet, the terminal voltage, and the electric fields of the Wien filters are then adjusted to allow the reference isotope Y to pass. The current of this isotope is measured using a Faraday cup in the dedicated AMS beam line (between the switching magnet and the third Wien filter; see Fig. 2). Afterwards, the beam line is set to a superheavy mass setting. Data are taken for this setting for an average of 2000 seconds. Then the beam line is set back to the reference isotope and the current is recorded again to obtain the average current during the superheavy run. The stability of the current can be

indirectly monitored by observing the count rate of background events in the detection system.

It is also important to know the total efficiency ϵ of the detection system. It is defined here as the probability that an ion that would be registered at the Faraday cup will be also registered in the silicon detector. By measuring the current of the reference isotope Y (with a number abundance n_Y in the sample material), such as ^{192}Os or ^{198}Pt, with the Faraday cup and comparing it to the count rate of that isotope in the detector after retracting the Faraday cup, and then attenuating the beam by a known factor (typically 10^6) to protect the silicon detector, the detection efficiency ϵ can be calculated. Typical values during the experiment were in the range $12.2\% \leqslant \epsilon \leqslant 31.5\%$. The variation in this value results mostly from different settings of the ion-optical elements of the beam line during different parts of the experiment.

By recording the reference current of the stable isotope Y with the charge state q before and after an AMS run of duration t with settings for a superheavy isotope X, the number of particles of species Y that could have been recorded and identified in the detector during the time t can be calculated with

$$ N_Y = \frac{\overline{I} \times t \times \epsilon}{e \times q}, \qquad (1) $$

where $\overline{I}$ denotes the average current of isotope Y during the run, e the elementary charge, and q the chosen charge state of isotope Y. If during the run no events of a superheavy isotope X were recorded, then an upper limit on the number abundance n_X of isotope X in the sample material can be calculated using

$$ n_X = \frac{1.29}{N_Y} \times \frac{S_Y}{S_X} \times n_Y, \qquad (2) $$

where S_X and S_Y are the stripping yields for the chosen charge states of isotopes X and Y (probability of the formation of the selected charge state during the stripping process in the tandem accelerator), respectively, n_Y is the abundance of the reference isotope, and the factor 1.29 includes a 1σ interval for the upper limit as suggested by Feldman and Cousins [19] for a background-free measurement.

Giving upper limits as described above using Eq. (2) however requires knowledge about all components of the sample material to determine n_Y. It is also useful to determine the resulting upper limits as mass fractions in the following form:

$$ m_X = \frac{1.29}{N_Y} \times \frac{S_Y}{S_X} \times \frac{A_X}{A_Y} \times m_Y, \qquad (3) $$

where m_X is the upper limit on the mass fraction of SHE Y and m_Y is the mass fraction of the reference isotope in the sample material.

It should be mentioned here that it is not possible with this setup to assign a specific atomic number Z to a possible SHE event, because the signals from isobars are indistinguishable. This means that without introducing additional assumptions, such as presuming the neutron number to be most likely the magic $N = 184$, we are always scanning for all possible isobars, which is actually an advantage because this search

is meant to be as widespread as possible. X thus denotes an isotope of an arbitrary SHE.

V. SYSTEMATIC UNCERTAINTIES

Since experimental data on SHEs are scarce, we need to make reasonable assumptions on their chemical behavior and physical properties.

A. Negative ion formation and reference isotopes

Equation (2) does not take the different abilities of isotopes X and Y to form negative ions in the ion source into account. This is primarily determined by the electron affinity of the element. Due to the lack of experimental data on electron affinities of SHEs, this uncertainty was not taken into account, but it requires some discussion. As was argued in Sec. II, the most likely SHEs to be found are the relatively light ones
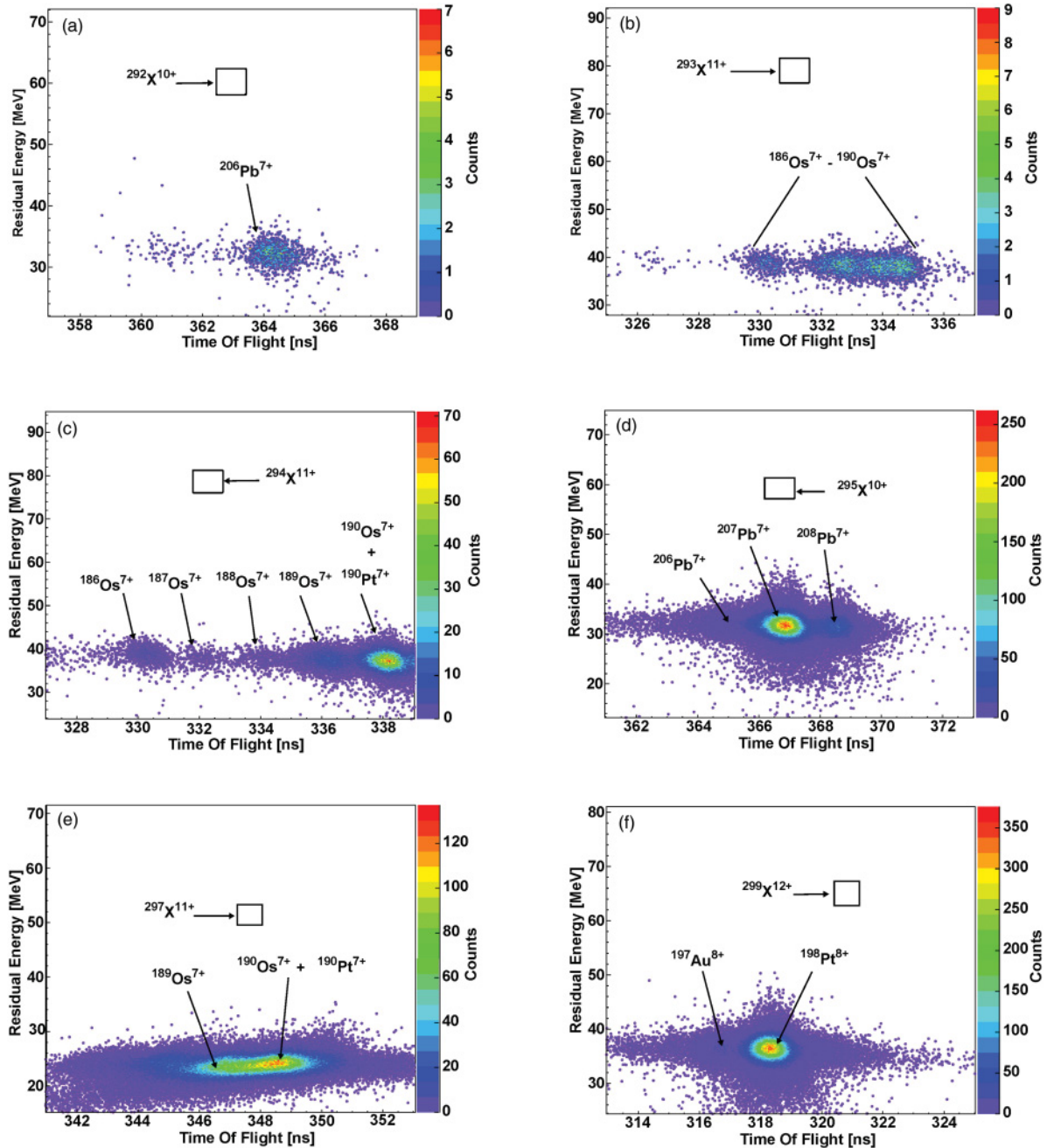

FIG. 3. (Color online) The spectra (a)–(f) show the signal of the silicon detector versus the time of flight for the mass settings 292 to 299 with the sample material raw platinum. They are zoomed in to the region of interest for the superheavy candidate, including the closest possible source for background events, typically isotopes in the charge states 7+ or 8+ which arrive at the detection system because of similar mass-to-charge ratios as the SHEs. All spectra show zero background in the regions where SHE events would be expected (boxed 1σ area around the calculated signal). While the count rate was relatively low for (a)–(e), the setting (f) ($A = 299$) had the highest count rate of the six settings, caused by ^{198}Pt^{8+} which is highly abundant in the sample material.

(Hs, Mt, Ds, and Rg). The electron affinity in the corresponding groups 8–11 of the periodic table increases in all four cases from period 5 to 6 and, except for group 10, also from period 4 to 5 as can be seen in Fig. 1. It is thus reasonable to assume

that SHEs would not perform worse than their homologues in the ion source.

It is favorable to use as a reference isotope an element that is chemically homologous to the SHE being sought. This was
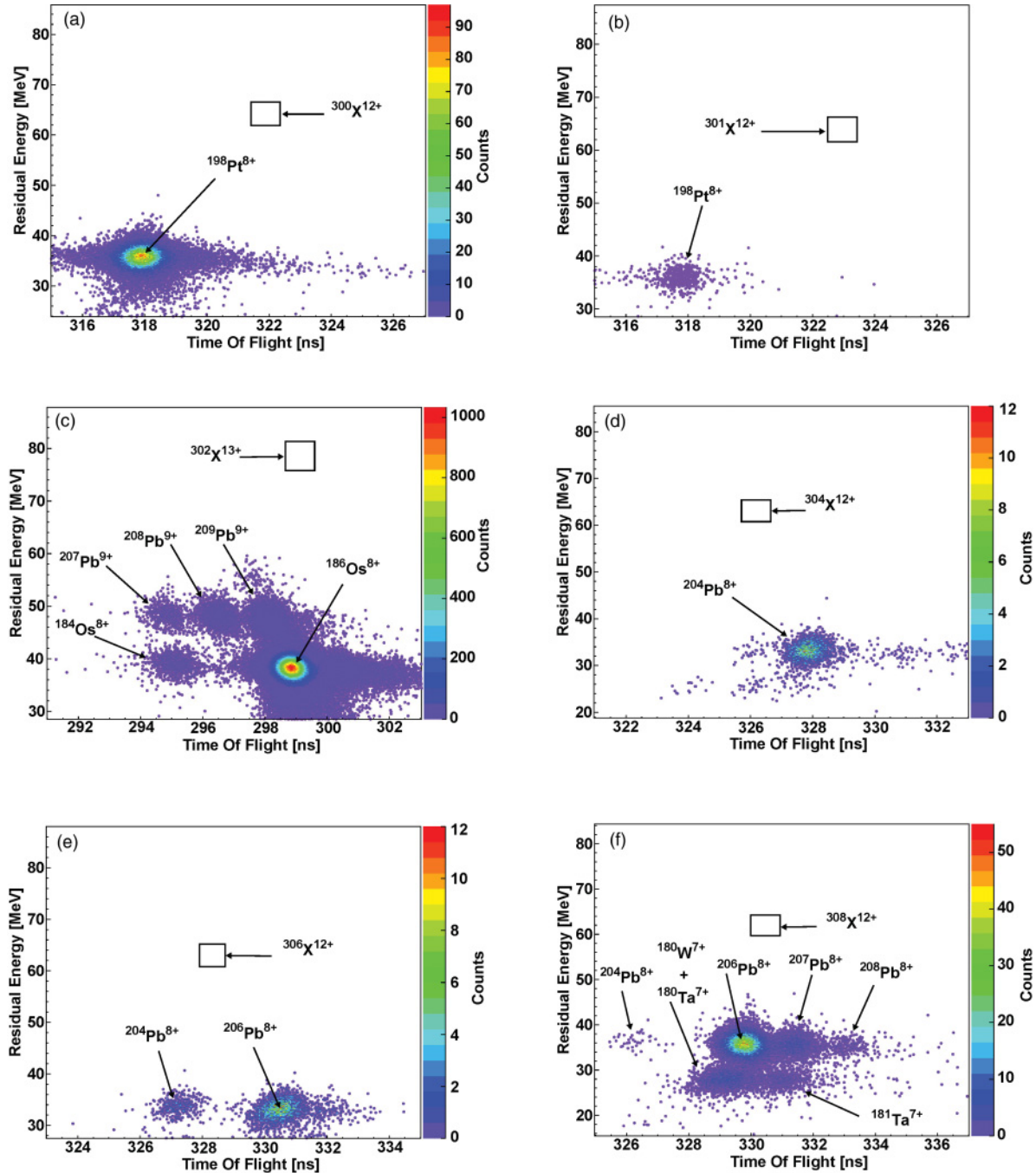

FIG. 4. (Color online) The spectra (a)–(f) show the signal of the silicon detector versus the time of flight for the mass settings 300 to 308 with the sample material raw platinum. They are zoomed in to the region of interest for the superheavy candidate, including the closest possible source for background events, typically isotopes in the charge states 7+ or 8+ which arrive at the detection system because of similar mass-to-charge ratios as the SHEs. All spectra show zero background in the regions where SHE events would be expected (boxed 1σ area around the calculated signal). The only case with a significantly high count rate was (c) ($A = 302$), where the count rate of $^{186}Os^{8+}$ was able to cause pile-up that could potentially cause background events in the expected region of $^{302}X^{13+}$, which was however suppressed by the pile-up rejection system.

attempted for ^{292}Hs, ^{294}Ds, and ^{298}114 with their most probable chemical homologues osmium, platinum, and lead, providing the reference isotopes ^{192}Os, ^{198}Pt, and ^{208}Pb. For all other SHEs, the reference isotope ^{198}Pt was also used. Naturally, this introduces a systematical error that is difficult to assess but cannot be avoided.

In all cases, except for $A = 298$, we attempted to extract the SHE X as the elemental ion X$^-$ from the ion source. As for $A = 298$, which was searched for in the sample material lead fluoride, both reference isotope ^{208}Pb and SHE ^{298}114 were extracted as trifluorides (PbF$_3^-$) because of the better performance in the ion source [20], under the assumption that the most likely SHE candidate with $A = 298$ is element 114 due to the neutron shell closure at $N = 184$.

B. Masses of SHEs

The precise masses of the SHEs in this work are experimentally unknown. Calculations by Smolanczuk [21] suggest a typical mass excess of about 0.2 amu in the SHE mass region under consideration in the experiment. The elements of the beam line were adjusted accordingly. However, a mass value different by 0.1 amu would still not influence the transmission through the beam transport system.

C. Stripping yields and charge states

The stripping yields of the selected charge states of the SHEs were calculated using the formulas provided by Sayer *et al.* [22]. For these calculations, the proton number for each mass setting A was chosen as $Z = A - 184$ because of the neutron shell closure $N = 184$. Although the stripping yield occurs in Eq. (1), maximizing it is not the only concern for choosing the charge state for the SHE candidates. It is also important to avoid overly high count rates in the silicon detector, first because this can produce pile-up, and second to prevent the silicon detector from being damaged. To this end, charge states that minimize the interference from isotopes abundant in the samples with similar mass-to-charge ratio m/q but still have a resonably large stripping yield (typically 17%) were chosen. In this experiment, the charge states for the SHEs ranged beween 10+ and 13+, resulting in kinetic energies between 95 and 150 MeV.
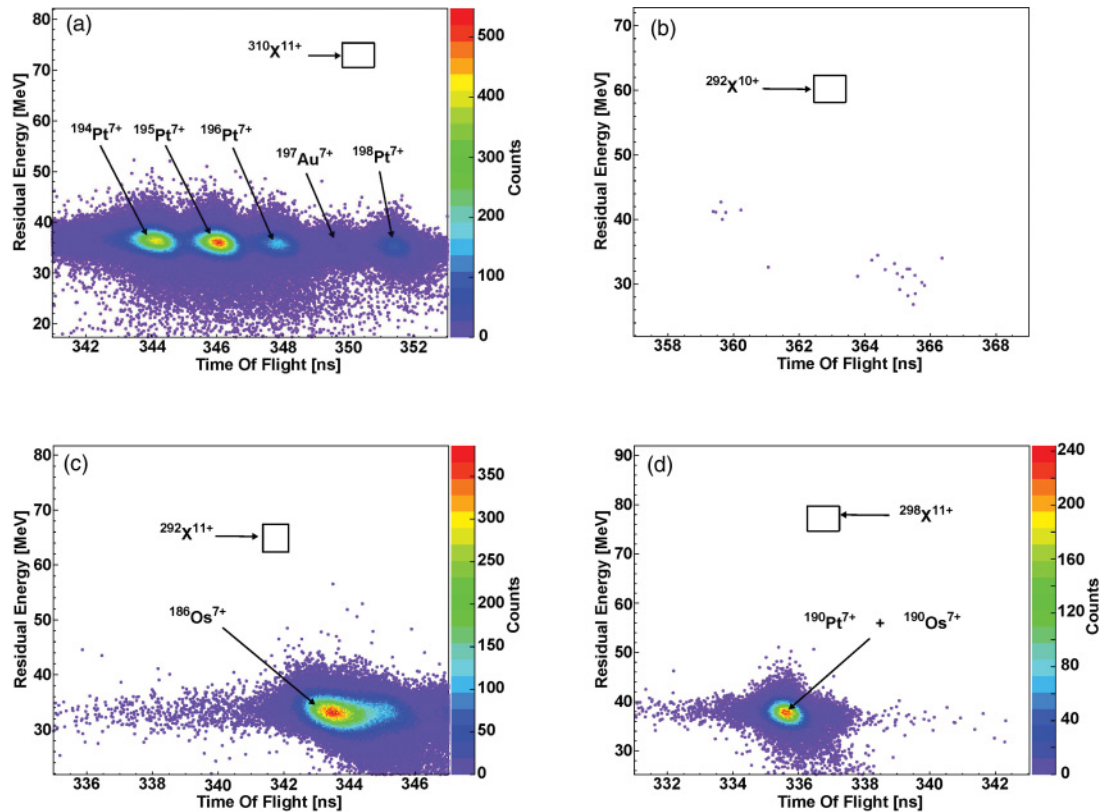

FIG. 5. (Color online) The spectra (a)–(d) show the signal of the silicon detector versus the time of flight for the following settings and sample materials: (a) $A = 310$ in raw platinum, (b) $A = 292$ in osmium in the charge state 10+, (c) $A = 292$ in osmium in the charge state 11+, and (d) $A = 298$ in lead fluoride. They are zoomed in to the region of interest for the superheavy candidate, including the closest possible source for background events, typically isotopes in the charge states 7+ or 8+ which arrive at the detection system because of similar mass-to-charge ratios as the SHEs. All spectra show zero background in the regions where SHE events would be expected (boxed 1σ area around the calculated signal). The cleanest spectrum (lowest count rate) that was recorded in the experiment was the case (b) (^{292}X^{10+}). However, a low, stable count rate in the detection system is desirable because it is an indirect check on the stability of the system (mostly the current extracted from the ion source) during runs. Thus, the charge state 11+ was also used; see (c).

TABLE I. The table shows, from left to right, the mass number of the SHE (A_{SHE}), the sample material in the ion source (Sample), the type and charge state of the reference isotope (Ref. isotope), its mass fraction (m_{ref}) and atom number fraction (n_{ref}) in the sample material, the charge state (q_{SHE}) of the SHE, the calculated stripping yields of the reference isotope (S_{ref}) and the SHE (S_{SHE}), and the experimental parameters: average current of the reference isotope ($\overline{I}$), measuring time (Time), detection efficiency (ϵ), the count rate in the silicon detector (Rate), and the SHE events (SHE ev.). Vertical gaps seprate the different sample materials. For $A = 292$ in the sample material osmium, two charge states were used (10+ had much lower count rate than 11+). For $A = 298$ in lead fluoride, the mass fraction of ^{208}Pb is given relative to lead, neglecting fluorine.

A_{SHE}	Sample	Ref. isotope	m_{ref} (%)	n_{ref} (%)	q_{SHE}	S_{ref} (%)	S_{SHE} (%)	$\overline{I}$ (nA)	Time (h)	ϵ (%)	Rate (Hz)	SHE ev.	Fig.
292	Os	^{192}Os^{9+}	41.37	41.0	11+	17.1	17.8	11.6	25.6	18.0	31	0	5(b)
292	Os	^{192}Os^{7+}	41.37	41.0	10+	14.4	19.1	11.1	10.6	26.4	0.01	0	5(c)
292	raw Pt	^{198}Pt^{7+}	2.35	0.70	10+	14.7	19.1	4.9	2.3	20.0	9	0	3(a)
293	raw Pt	^{198}Pt^{7+}	2.35	0.70	11+	14.7	18.4	8.7	3.4	31.5	2	0	3(b)
294	raw Pt	^{198}Pt^{7+}	2.35	0.70	11+	14.7	18.5	2.8	9.7	31.5	17	0	3(c)
295	raw Pt	^{198}Pt^{7+}	2.35	0.70	10+	14.7	18.9	6.8	7.1	31.0	6	0	3(d)
297	raw Pt	^{198}Pt^{8+}	2.35	0.70	11+	16.7	17.7	5.0	5.0	12.4	6	0	3(e)
298	PbF$_2$	^{208}Pb^{7+}	52.59	52.4	11+	18.3	16.2	13.1	5.2	19.6	11	0	5(d)
299	raw Pt	^{198}Pt^{8+}	2.35	0.70	12+	16.7	16.0	2.6	3.3	12.2	81	0	3(f)
300	raw Pt	^{198}Pt^{8+}	2.35	0.70	12+	16.7	16.1	5.7	2.2	16.4	7	0	4(a)
301	raw Pt	^{198}Pt^{8+}	2.35	0.70	12+	16.7	16.1	3.0	1.8	12.5	1	0	4(b)
302	raw Pt	^{198}Pt^{8+}	2.35	0.70	13+	16.7	14.0	6.3	2.5	20.5	50	0	4(c)
304	raw Pt	^{198}Pt^{8+}	2.35	0.70	12+	16.7	16.1	2.0	4.2	12.5	2	0	4(d)
306	raw Pt	^{198}Pt^{8+}	2.35	0.70	12+	16.7	17.6	2.8	3.6	12.8	8	0	4(e)
308	raw Pt	^{198}Pt^{8+}	2.35	0.70	12+	16.7	16.1	1.1	1.7	12.9	136	0	4(f)
310	raw Pt	^{198}Pt^{7+}	2.35	0.70	11+	14.7	18.0	4.9	6.2	29.1	33	0	5(a)

VI. RESULTS AND DISCUSSION

For this experiment, a total of 72 hours of data were taken in three separate beam times in 2010. Spectra for all examined masses can be seen in Figs. 3–5. The spectra show the signals of the silicon detector (residual energy) versus the time of flight. All events that were registered in the detector due to similar values of p/q, and thus are not completely suppressed by the 90° magnet and the Wien filters, could be clearly distinguished from possible SHE events. This is a result of their lower-energy deposition in the silicon detector, because of their lower kinetic energy obtained in the tandem accelerator due to their lower charge states. The figures include 1σ boxes around the expected signal of the SHE in question. It should be mentioned here that the expected TOF for SHEs can be easily calculated because of the well defined energy, while the expected residual energy measured in the silicon detector depends on the energy loss in the detector gas and thus on the proton number Z of the SHE. The expected residual energies are thus not as well defined as the TOF signals. This implies that if events occurred slightly below or above the box, they would require additional analysis (e.g., examination of the corresponding ΔE signals) to identify them as SHE signals or not.

The events that were registered in the detector typically correspond to isotopes that are abundant in the sample material. However, even small contaminations or crosstalk of samples (contamination of the ion source by prolonged exposure to a certain element) can cause additional sources of background count rate. In Fig. 5(d), a large contribution to the count rate came from isotopes with $A = 190$, although the sample material PbF$_2$ mixed with silver powder did not contain platinum or osmium abundantly.

There were no SHE events recorded for any of the mass settings. The results are summarized in Table I. Using Eqs. (1)–(3), upper limits for the abundances of SHEs with the examined masses can be calculated, and are given in Table II. Note that,

TABLE II. Overview on the obtained upper limits on the abundances and mass fractions of the SHEs in the respective sample materials calculated on a 1σ confidence level. X stands for an arbitrary SHE. Due to the known concentrations of Ir, Pt, and Au in the raw platinum, the upper limits for the possible chemical homologue elements Mt, Ds, and Rg could also be calculated.

Ratio	Sample	Upper limit $\left[\frac{\text{atoms}}{\text{atoms}}\right]$	Upper limit $\left[\frac{\text{g}}{\text{g}}\right]$
^{292}Hs/Os	Os	2.0×10^{-15}	3.0×10^{-15}
^{292}X/raw Pt	raw Pt	9.4×10^{-16}	4.8×10^{-15}
^{293}Mt/Ir	raw Pt	3.6×10^{-14}	5.4×10^{-14}
^{293}X/raw Pt	raw Pt	2.4×10^{-16}	1.2×10^{-15}
^{294}Ds/Pt	raw Pt	2.7×10^{-15}	4.0×10^{-15}
^{294}X/raw Pt	raw Pt	2.6×10^{-16}	1.3×10^{-15}
^{295}Rg/Au	raw Pt	4.1×10^{-14}	6.1×10^{-14}
^{295}X/raw Pt	raw Pt	1.5×10^{-16}	7.3×10^{-16}
^{297}X/raw Pt	raw Pt	9.9×10^{-16}	4.9×10^{-15}
^{298}Uuq/Pb	PbF$_2$	1.8×10^{-14}	2.6×10^{-14}
^{299}X/raw Pt	raw Pt	3.2×10^{-15}	1.6×10^{-14}
^{300}X/raw Pt	raw Pt	1.6×10^{-15}	8.2×10^{-15}
^{301}X/raw Pt	raw Pt	4.9×10^{-15}	2.5×10^{-14}
^{302}X/raw Pt	raw Pt	1.2×10^{-15}	6.1×10^{-15}
^{304}X/raw Pt	raw Pt	3.2×10^{-15}	1.6×10^{-14}
^{306}X/raw Pt	raw Pt	2.4×10^{-15}	1.2×10^{-14}
^{308}X/raw Pt	raw Pt	1.4×10^{-14}	7.2×10^{-14}
^{310}X/raw Pt	raw Pt	2.6×10^{-16}	1.4×10^{-15}

for the material raw platinum, not only the abundance of a SHE in the sample material, but also that SHE's abundance in a possibly chemical homologue material—which is present in the sample as indicated in Fig. 1—can be calculated. Thus, additional limits are given for the abundances of the possibly chemically homologous elements Mt in Ir, Ds in Pt, and Rg in Au.

The lack of events that could be attributed to SHEs can have several reasons. First, the *r* process might simply be unable to produce SHEs in sufficient amounts. Second, the half-lives of SHEs could be so short that their abundance in the samples has dropped below our detection limits in the time since their synthesis until today. Also, it cannot be excluded that, instead of following their expected chemical homologues, geochemical processes might have separated SHEs from our sample materials.

Nonetheless, it was demonstrated, that the setup is able to clearly distinguish any background events from possible SHE signals due to the high charge states used, which are basically determined by the available terminal voltage. This allows for very clean measurements.

VII. SUMMARY AND OUTLOOK

In this experiment, a total of 14 different masses in the range $292 \leqslant A \leqslant 310$ were scanned with AMS. No events could be attributed to SHEs. The resulting upper limits on their abundances in the sample materials are of the order 10^{-14}–10^{-16}. It has been shown that AMS is uniquely suited to search for SHEs, not only in this paper, but also recently by the VERA AMS group in Vienna, who performed similar

experiments with the sample materials gold, platinum, lead, and bismuth [23,24], and reached upper limits comparable to ours. These upper limits are lower than those of comparable, earlier searches with AMS [25] and other techniques such as neutron counting [26,27], which demonstrates that the current AMS experiments are a very efficient means for SHE searches in nature. It should also be emphasized again that AMS does not have to deal with molecular background, unlike other mass spectrometry methods such as ICPMS. Also, it is not necessary to assume a maximum half-life, as in decay counting experiments.

For the future, it would not be easy to improve the upper limits in Table II by a large factor, because of the limited measuring times and currents, but there are other possibilities to explore. The most interesting objective for the future of the project will be to extend the search to other promising sample materials.

[1] Y. T. Oganessian *et al.*, Phys. Rev. C **74**, 044602 (2006).

[2] U. Mosel and W. Greiner, Z. Phys. **222**, 261 (1969).

[3] E. O. Fiset and J. Nix, Nucl. Phys. A **193**, 647 (1972).

[4] J. M. Gates *et al.*, Phys. Rev. C **83**, 054618 (2011).

[5] Y. T. Oganessian, J. Phys. G: Nucl. Part. Phys. **34**, R165 (2007).

[6] I. Panov, I. Y. Korneev, and F.-K. Thielemann, Phys. At. Nucl. **72**, 1026 (2009).

[7] P. R. Chowdhury, C. Samanta, and D. N. Basu, Phys. Rev. C **77**, 044603 (2008).

[8] R. K. Gupta, Niyti, M. Manhas, and W. Greiner, J. Phys. G: Nucl. Part. Phys. **36**, 115105 (2009).

[9] A. Marinov, I. Rodushkin, D. Kolb, A. Pape, Y. Kashiv, R. Brandt, R. V. Gentry, and H. W. Miller, Int. J. Mod. Phys. E **19**, 131 (2010).

[10] F. Dellinger, O. Forstner, R. Golser, W. Kutschera, A. Priller, P. Steier, A. Wallner, and G. Winkler, Nucl. Instrum. Methods Phys. Res., Sect. B **268**, 1287 (2010).

[11] Impala Platinum Holdings Limited, No. 2 Fricker Road, Illovo 2196, South Africa, [www.implats.co.za].

[12] Alfa Aesar GmbH & Co. KG, A Johnson Matthey Company, Postfach 110765, 76057 Karlsruhe, Germany.

[13] M. Schädel and A. Türler, J. Phys. **8**, 30 (2009).

[14] C. E. Düllmann *et al.*, Nature (London) **418**, 859 (2002).

[15] R. Middleton, *A Negative-Ion Cookbook* (University of Pennsylvania, Philadelphia, 1990).

[16] A. Urban, G. Korschinek, and E. Nolte, in *Proceedings of the Workshop on Techniques in Accelerator Mass Spectrometry,*

Oxford, 1986, edited by R. E. M. Hedges and E. T. Hall (Oxford Radiocarbon Accelerator Unit, Oxford, 1986), p. 108.

[17] K. Knie, T. Faestermann, and G. Korschinek, Nucl. Instrum. Methods Phys. Res., Sect. B **123**, 128 (1997).

[18] C. Wallner, T. Faestermann, U. Gerstmann, W. Hillebrandt, K. Knie, G. Korschinek, C. Lierse, C. Pomar, and G. Rugel, Nucl. Instrum. Methods Phys. Res., Sect. B **172**, 333 (2000).

[19] G. J. Feldman and R. D. Cousins, Phys. Rev. D **57**, 3873 (1998).

[20] G. Korschinek, J. Sellmair, A. Urban, and M. Müller, Nucl. Instrum. Methods Phys. Res., Sect. A **271**, 328 (1988).

[21] R. Smolanczuk, Phys. Rev. C **56**, 812 (1997).

[22] R. O. Sayer, Rev. Phys. Appl. **12**, 1543 (1977).

[23] F. Dellinger, W. Kutschera, O. Forstner, R. Golser, A. Priller, P. Steier, A. Wallner, and G. Winkler, Phys. Rev. C **83**, 015801 (2011).

[24] F. Dellinger, O. Forstner, R. Golser, A. Priller, P. Steier, A. Wallner, G. Winkler, and W. Kutschera, Phys. Rev. C **83**, 065806 (2011).

[25] W. Stephens, J. Klein, and R. Zurmühle, Phys. Rev. C **21**, 1664 (1980).

[26] D. A. Testov, C. Briançon, S. N. Dmitriev, A. V. Yeremin, Y. E. Penionzhkevich, Y. V. Pyatkov, and E. A. Sokol, Phys. At. Nucl. **72**, 1 (2009).

[27] A. Svirikhin, C. Briançon, S. N. Dmitriev, Y. T. Oganessian, E. A. Sokol, D. A. Testov, and A. V. Yeremin, AIP Conf. Proc. **1175**, 297 (2009).